Energy 71 (2014) 638–644

Contents lists available at ScienceDirect

Energy

journal homepage: www.elsevier.com/locate/energy

Downdraft gasification of corn straw as a non-woody biomass: Effects of operating conditions on chlorides distribution

Chao Gai, Yuping Dong*, Tonghui Zhang

Key Laboratory of High Efficiency and Clean Mechanical Manufacture, Department of Mechanical Engineering, Shandong University, Jinan 250061, PR China

ARTICLE INFO

Article history:
Received 6 December 2013
Received in revised form
27 April 2014
Accepted 3 May 2014
Available online 2 June 2014

Keywords:
Corn straw
Non-woody biomass
Downdraft
Gasification
Chlorine
Response surface methodology

ABSTRACT

The study concerns the distribution of chlorine species in the gaseous phase and the condensed phase during gasification of corn straw. The gasification of corn straw was carried out in a downdraft fixed bed gasifier using air and steam as gasifying agents. The effects of the air equivalence ratio (ER) for corn straw, steam to biomass mass ratio (SB), biomass particle size (PS) and their interactions on the distribution of chlorides were investigated using response surface methodology (RSM). The results indicate that ER and SB have a major effect on the distribution of gaseous chlorides, while ER and PS play the major role in affecting the distribution of chlorine retained in the condensed phase.

© 2014 Elsevier Ltd. All rights reserved.

1. Introduction

Energy crisis and the problems of environmental pollution during the over exploration of fossil fuels have intensified in recent decades [1–4]. As estimated by U.S. Department of Energy's Biomass Program [5], the vast agricultural and forest biomass resources have the potential to provide a source of biofuels with the development of advanced conversion technology, whilst protecting ecological resources and enhancing ecosystem services. As a typical technology of converting biomass to sustainable biofuels, gasification involves high temperature (600–900 °C or even higher) partial oxidation of biomass with gasifying agents (e.g., air, oxygen, steam and CO_2) to produce raw gas with low-to-medium heating value for the biofuel production [6–9].

The raw gas obtained during gasification is mainly composed of CH_4, CO, CO_2, H_2, H_2O and hydrocarbon gases. However, it also contains minor contaminations in terms of tars, sulfides, chlorides, and alkali metals [10–12]. This will be detrimental to reactors, purification and conditioning systems. Apart from gaseous chlorides, chlorine will react with alkali metals (i.e. potassium, sodium) in the feedstock to produce alkali species. These compounds are partly bounded to the ash surface, which will bring about sintering or bed agglomeration. It can result in the unstable bed operation and damage to reactors and downstream equipments. Compared with woody biomass, a higher concentration of chlorine can be observed in the fast-growing non-woody biomass such as grass and straw [13,14]. As already discussed in a previous paper [15], the product gas obtained from gasification of non-woody biomass has a relatively high concentration of chlorine species compared with the gasification of woody biomass. According to Porbatzki et al. [16], generally the amount of inorganic trace elements released from the herbaceous biomass was about one order of magnitude higher than from the woody biomass. Therefore, in respect to this significant issue during gasification of non-woody biomass, researchers have focused on the methods for inhibiting or removing chlorine species during the gasification process such as leaching of feedstock [17], catalysts or sorbents [18], and co-gasification [19].

Although there have been some experimental investigations concerning the release and removal of chlorine in the product gas from biomass gasification, few reports are available on the interactions of varied operating conditions on minimizing chlorine emissions during the gasification process. Besides, the traditional one-factor-at-a-time method has been applied in most studies of biomass gasification. This method could not investigate the interactions of different operating parameters on the desired experimental results. Consequently, response surface methodology (RSM) [20] was adopted in the current study in view of the fault of the classical method. It can reduce the number of experimental

---

* Corresponding author. Tel.: +86 531 88392199; fax: +86 531 88373588.
E-mail address: dongyp@sdu.edu.cn (Y. Dong).

http://dx.doi.org/10.1016/j.energy.2014.05.009
0360-5442/© 2014 Elsevier Ltd. All rights reserved.

runs and can be used to quantitatively determine the relationships between one or more response variables and a number of independent variables. Therefore, the main objective of this study is to investigate the effect of the air equivalence ratio (ER), steam to biomass mass ratio (SB) and biomass particle size (PS) and their interactions on the distribution of chlorides during the gasification of non-woody biomass. It is hoped that the result obtained in the current study can give a better and more comprehensive understanding of the releasing mechanisms of chloride pollutants during the gasification of non-woody biomass.

2. Experimental methods

2.1. Raw material

Corn straw was selected as the feedstock for its relatively high amount of chlorine compared with woody biomass. The samples were first air-dried for 30 days to reduce the moisture content to less than 10%. Then after being crushed and sieved, three fractions of particle size were chosen for the experimental runs, including 2.5 ± 0.09 mm, 5.5 ± 0.22 mm and 8.5 ± 0.26 mm. The samples after the pretreatment were stored under dry conditions at the room temperature. For each particle size, the proximate and ultimate analyses of the sample were conducted according to the same methods described in the previous study [15]. The average results are summarized in Table 1. The samples with different particle sizes have the same composition within a normal variation.

2.2. Experimental procedure

Chlorine is released in two principal chemical forms, including gaseous compounds in the product gas and bounded to the solid ash during the gasification of non-woody biomass. Besides gaseous chlorine hydride (HCl), chlorine will react with alkali metals such as potassium and sodium, which are the major sources of alkali in most biomass. Then a certain amount of alkali chlorides will be evaporated to gaseous chlorine compounds at high temperatures during the gasification. According to the chemical equilibrium model established by Turn [21], the potassium and sodium are primarily present as chlorides (KCl and NaCl) and a small amount of chloride dimers (e.g., $(KCl)_2$ and $(NaCl)_2$). Therefore, the major chlorine compounds of HCl, KCl and NaCl in fuel gas were selected in this study to investigate the distribution of chlorine in the gaseous phase during the gasification process.

Experiments were all conducted on a bench-scale downdraft fixed bed gasification system. The scheme diagram of the experimental system is demonstrated in Fig. 1. It is mainly composed of a downdraft fixed bed gasifier, control and measurement systems. The gasifier is a cylindrical reactor with an internal diameter of 0.3 m and a total height of 0.85 m. An induced-draft fan is installed at the upper part of the reactor. An agitator is mounted on the induced-draft fan to agitate the feedstocks in the reactor, reinforcing gas–solid reaction and avoiding the partial ash sintering on the wall. The center air distribution nozzle is installed at the bottom of the induced-draft fan, maintaining a base level with nine equally distributed bustle pipes. A perforated, cast iron rotating grate is installed at the bottom of the reactor to dispose the ash continuously from the bed. Ash hopper 1 is used to collect the bottom ash from the gasifier, while the fly ash in product gas was collected in ash hopper 2. The temperature profiles along the reactor vertical axis were measured by two K-type and three N-type thermocouples installed at five points along the reactor vertical axis. In addition, the temperature profiles of the gasifier throat and two ash hoppers were also measured. During each test, the biomass feed rate was adjusted to the desired value by a screw feeder. The air flow rate was adjusted by the valve of the air supply. The steam flow rate was adjusted by a frequency controller of the water pump.

Table 1
Proximate and ultimate analysis of the corn straw.

Proximate (wt% db[a])	Mean	Ultimate (wt% daf[b])	Mean	Ultimate (wt% daf[b])	Mean
Volatile matter	75.95	Carbon	43.83	Sulfur	0.13
Fixed carbon	13.75	Hydrogen	5.95	Chlorine	0.49
Ash	5.93	Oxygen	45.01	Potassium	0.23
Moisture (ar[c])	6.17	Nitrogen	0.97	Sodium	0.02

[a] Dry basis.
[b] Dry ash free basis.
[c] As received basis.

The chlorine species were sampled and analyzed when the reactor had reached a steady-state (i.e. the temperatures in both the partial oxidation zone and the reduction zone were nearly constant). In respect to the sampling of gaseous chlorides, the raw gas was continuously extracted from the gas outlet of the cyclone. The dedusted product gas downstream the cyclone was drawn by a vacuum pump through two 250 ml impinger bottles containing 0.01 M NaOH solution to neutralize HCl for 0.5 h. Then the HCl content in the solvents was off line determined with the silver nitrate titration method [22]. Besides, the raw gas obtained from the gas outlet of the cyclone was washed with distilled water to measure the content of KCl and NaCl. The four absorbing bottles were all kept in an ice bath. Then the liquid samples collected in a flask were analyzed via Inductively Coupled Plasma Optical Emission Spectrometry (ICP-OES) (2000DV, PerkinElmer Corp., USA). In terms of the measurement of the chlorine species bounded to the solid ash during the gasification process, the ash hopper 1 located at the bottom of the gasifier was used to collect the bottom ash samples whilst the ash hopper 2 at the bottom of the cyclone was used to collect the fly ash samples entrained with the product gas. After that, the amount of chlorine in the solid ash samples collected from two ash hoppers was analyzed by an elementary analyzer (vario MACRO cube, ELEMENTAR) using a thermal conductivity detector and operating in the mode of Carbon (C), Hydrogen (H), Nitrogen (N) and Sulfur (S). Helium was selected as the carrier gas in all analyses.

2.3. Experimental design

Response surface methodology (RSM) is used to investigate the interactions of independent factors to the response variables. ER, SB and PS greatly affect the distribution of chlorine species during gasification of non-woody biomass. Therefore, the three operating parameters were selected as independent factors. The ranges of three independent factors are 0.2–0.4 for ER, 0.8–1.6 for SB and 2.5–8.5 mm for PS. To reach the designed levels of ER and SB, the biomass feed rate was kept at 9.0 kg/h. The air flow rate was adjusted from 12.6 to 25.2 Nm^3/h while the steam flow rate was varied from 7.2 to 14.4 kg/h. As introduced in the section of Experimental methods that the response variables investigated were: HCl, KCl, NaCl and the chlorine bounded in the bottom ash and the fly ash. In this study, a face-centered central composite design (FCCCD) was used to build the surface model. Based on the number of independent variables and corresponding levels, three types of experimental runs, including eight factorial points, six axial points, and six central points were performed. Table 2 presents the complete design matrix and

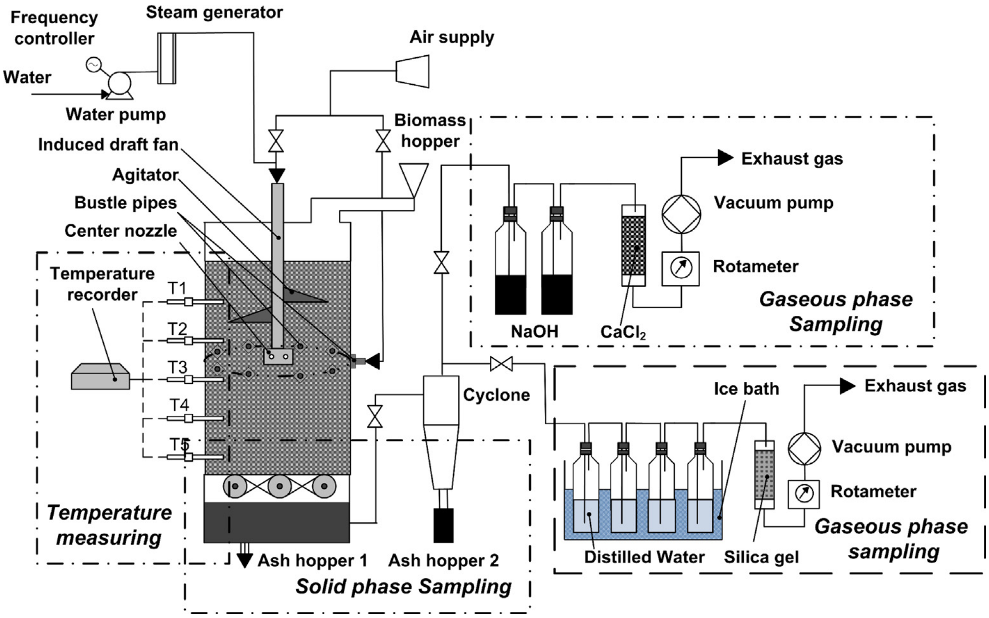

Fig. 1. Scheme diagram of the downdraft fixed bed experimental system.

actual response variables of the experiments conducted in the current study. To rule out experimental bias or random error, once a day, three independent experiments for each condition were performed on three days. And each sample from each test was measured for three times. The average values and standard deviations are both reported in Table 2.

3. Results and discussion

3.1. Model fitting and validation

Based on the experimental results shown in Table 2, second-order polynomial regression analysis was used to fit the response variables to the experimental data. The models developed for the distribution of chlorides are shown as below.

$$\begin{aligned}\text{HCl} = {} & 2663.79 + 1187.96{*}X_{ER} - 303.29{*}X_{SB} - 148.73{*}X_{PS} \\ & + 141.38{*}X_{ER}{*}X_{SB} + 132.36{*}X_{SB}{*}X_{PS} - 433.85{*}X_{ER}^2 \\ & + 379.52{*}X_{SB}^2\end{aligned} \tag{1}$$

$$\begin{aligned}\text{KCl} = {} & 1519.89 - 1157.18{*}X_{ER} - 471.23{*}X_{SB} - 271.09{*}X_{ER}{*}X_{SB} \\ & + 152.78{*}X_{ER}{*}X_{PS} + 415.28{*}X_{ER}^2 + 365.71{*}X_{SB}^2\end{aligned} \tag{2}$$

$$\begin{aligned}\text{NaCl} = {} & 237.42 + 163.28{*}X_{ER} - 38.79{*}X_{SB} - 14.18{*}X_{ER}{*}X_{SB} \\ & + 21.38{*}X_{ER}{*}X_{PS} + 13.19{*}X_{SB}{*}X_{PS} - 17.19{*}X_{ER}^2 \\ & + 49.50{*}X_{SB}^2\end{aligned} \tag{3}$$

$$\begin{aligned}\text{Cl in bottom ash} = {} & 1024.73 - 457.91{*}X_{ER} - 51.39{*}X_{SB} \\ & - 135.82{*}X_{PS} - 67.18{*}X_{ER}{*}X_{PS} \\ & - 42.39{*}X_{SB}{*}X_{PS} - 186.75{*}X_{ER}^2 \\ & - 56.36{*}X_{SB}^2 + 133.73{*}X_{PS}^2\end{aligned} \tag{4}$$

$$\begin{aligned}\text{Cl in fly ash} = {} & 2672.37 - 879.97{*}X_{ER} + 124.85{*}X_{SB} \\ & + 247.52{*}X_{PS} - 53.19{*}X_{ER}{*}X_{SB} \\ & - 129.08{*}X_{ER}{*}X_{PS} + 231.79{*}X_{ER}^2 - 201.57{*}X_{SB}^2 \\ & + 176.97{*}X_{PS}^2\end{aligned} \tag{5}$$

To evaluate the robustness of the fitting models, additional experimental points were investigated, which were not located in the experimental design matrix. Table 3 indicated that the experimental results agreed well with the predicted values. Attention should be given that the developed models are precise only on the specific reactor and feedstock that were investigated in this study. Nevertheless, the effect of operating conditions and their interactions on the distribution of chlorides can be properly evaluated based on the fitting models.

3.2. Chlorides released in the gaseous phase

3.2.1. Chlorine hydride

Fig. 2 demonstrates the response surfaces of HCl for different levels of independent factors. It indicates that the equivalence ratio and steam to biomass mass ratio are the two influential factors, while the factor of biomass particle size is comparatively less significant. This response variable also depends significantly on the interactions between the equivalence ratio and steam to biomass mass ratio, due to the large curvature of the response surfaces.

At any levels of SB, the concentration of HCl increased dramatically first with increasing the ER from 0.2 to 0.4, then accompanied by a slow increase and reaching a plateau. In our previous study [8], it was observed that the gasifier temperature increased steadily with increasing the ER. At lower ERs, HCl is released primarily during the devolatilization phase with high water-vapor concentration in the gas phase, which is brought by the relatively low-oxygen environment caused by lower ERs. Besides, a certain amount of gaseous KCl and NaCl will react with the steam to produce HCl by the reaction of (R1) and (R2) listed below. At higher ERs, the equilibrium of the reaction (R1) and (R2) is shifted to the

Table 2
FCCCD matrix of independent factors and response variables.

Run no.	Point type	ER	SB	PS (mm)	Temp (°C)	HCl (ppmv)	KCl (ppmv)	NaCl (ppmv)	Cl in bottom ash (mg/kg)	Cl in fly ash (mg/kg)
1	Factorial	0.2 (−1)	0.8 (−1)	2.5 (−1)	1085.1	1703 ± 72	1198 ± 13	94 ± 1.2	1261 ± 18.8	3337 ± 101
2	Factorial	0.2 (−1)	0.8 (−1)	8.5 (+1)	1052.3	1143 ± 24	699 ± 20	38 ± 1.6	1356 ± 65.8	3780 ± 98
3	Factorial	0.4 (+1)	0.8 (−1)	2.5 (−1)	985.3	3572 ± 99	3748 ± 153	399 ± 10.8	390 ± 4.2	1986 ± 72
4	Factorial	0.4 (+1)	0.8 (−1)	8.5 (+1)	1008.9	3399 ± 245	3818 ± 208	430 ± 20.1	276 ± 14.5	1863 ± 128
5	Factorial	0.2 (−1)	1.6 (+1)	2.5 (−1)	1163.9	568 ± 10	655 ± 10	21 ± 0.4	1475 ± 36.3	4059 ± 73
6	Factorial	0.2 (−1)	1.6 (+1)	8.5 (+1)	1174.4	532 ± 22	479 ± 14	19 ± 0.9	1458 ± 108.1	4167 ± 161
7	Factorial	0.4 (+1)	1.6 (+1)	2.5 (−1)	1137.5	2994 ± 109	2096 ± 50	275 ± 6.7	828 ± 24.2	2446 ± 81
8	Factorial	0.4 (+1)	1.6 (+1)	8.5 (+1)	1156.2	3352 ± 278	2547 ± 182	356 ± 19.5	493 ± 30.5	2095 ± 175
9	Axial	0.3 (0)	0.8 (−1)	5.5 (0)	1035.2	3374 ± 207	2395 ± 81	337 ± 18.1	829 ± 32.3	2175 ± 114
10	Axial	0.3 (0)	1.6 (+1)	5.5 (0)	1164.1	2699 ± 90	1389 ± 19	232 ± 6.1	1211 ± 22.2	2830 ± 73
11	Axial	0.3 (0)	1.2 (0)	2.5 (−1)	1116.7	2322 ± 66	1216 ± 50	182 ± 1.7	1148 ± 14.1	2905 ± 108
12	Axial	0.3 (0)	1.2 (0)	8.5 (+1)	1108.8	2095 ± 128	1056 ± 71	154 ± 7.4	1207 ± 81.9	3056 ± 211
13	Axial	0.2 (−1)	1.2 (0)	5.5 (0)	1151.7	961 ± 32	758 ± 18	49 ± 1.5	1369 ± 16.6	3898 ± 122
14	Axial	0.4 (+1)	1.2 (0)	5.5 (0)	1109.8	3489 ± 91	3125 ± 100	386 ± 3.5	351 ± 4.0	1973 ± 61
15	Central	0.3 (0)	1.2 (0)	5.5 (0)	1116.8	2698 ± 48	1542 ± 40	230 ± 4.3	998 ± 11.7	2672 ± 62
16	Central	0.3 (0)	1.2 (0)	5.5 (0)	1132.2	2632 ± 99	1512 ± 58	249 ± 5.9	1002 ± 22.6	2584 ± 105
17	Central	0.3 (0)	1.2 (0)	5.5 (0)	1128.8	2715 ± 104	1514 ± 65	228 ± 8.6	1019 ± 39.9	2599 ± 113
18	Central	0.3 (0)	1.2 (0)	5.5 (0)	1152.1	2609 ± 172	1535 ± 129	241 ± 13.2	1017 ± 38.1	2731 ± 219
19	Central	0.3 (0)	1.2 (0)	5.5 (0)	1109.2	2670 ± 215	1481 ± 91	240 ± 10.0	1023 ± 34.7	2639 ± 204
20	Central	0.3 (0)	1.2 (0)	5.5 (0)	1146.3	2653 ± 65	1507 ± 63	239 ± 8.7	1011 ± 27.7	2643 ± 92

Biomass feed rate: 9.0 kg/h; air flow rate: 12.6–25.2 Nm^3/h; steam flow rate: 7.2–14.4 kg/h.

left. In addition, a certain amount of Cl_2 will be formed via the Deacon reaction (R3) [23] under the influence of more oxygen-containing functional groups at higher ERs. As suggested by Pinto et al. [24], chlorine may also be retained by some trace elements like Ca, Fe due to the reactions (R4) and (R5). Therefore, the content of HCl reached a plateau at higher ERs after a period of a rapid rise.

$$KCl\ (g) + H_2O \leftrightarrow KOH\ (g) + HCl\ (g) \tag{R1}$$

$$NaCl\ (g) + H_2O \leftrightarrow NaOH + HCl\ (g) \tag{R2}$$

$$2HCl + (1/2)O_2 \rightarrow Cl_2 + H_2O \tag{R3}$$

$$MO + 2HCl \leftrightarrow MCl_2 + H_2O \tag{R4}$$

$$M(OH)_2 + 2HCl \leftrightarrow MCl_2 + 2H_2O \tag{R5}$$

It can also be observed from Fig. 2 that the concentration of HCl slightly decreased with increasing the level of SB at lower ERs; whilst it rose again after a fall with increasing the level of SB at higher ERs. It suggests that the interactions between ER and SB seem could shift the equilibrium of formation and reduction of HCl at different bed temperatures, which should not be neglected. In addition, the concentration of HCl decreased with increasing the biomass particle size at higher ERs. It can be explained that the retention time of chlorine species on solid bed or ash is longer that reduces the HCl emission, because larger feedstock particles have greater heat transmission resistance and a lower surface area compared with smaller particles. Wei et al. [25] investigated the gasification of Swedish wood by the chemical equilibrium calculating tool. It was concluded that increasing the equivalence ratio increased the release of HCl, which is consistent with the results in the current study. However, Aljbour and Kawamoto [26] investigated the effect of operational conditions on contaminants released in bench-scale gasification of cedar wood. It was observed that the concentration of HCl in the product gas showed a slight decrease with increasing the equivalence ratio. It can be seen that the evolution of HCl is a complex issue, which is affected by the equilibrium of multiple reversible reactions. The discrepancies between results obtained by different investigations are not uncommon, and the reaction pathways of HCl are recommended for a further study.

3.2.2. *Potassium chloride*

Apart from a high concentration of chlorine released during the gasification of non-woody biomass, high amounts of potassium can also be detected. According to Porbatzki et al. [16], KCl is the thermodynamically preferred species rather than potassium hydroxide in case of the herbaceous biomass. It is verified by the molecular beam mass spectrometry (MBMS) measurement of the vaporized amount of KCl^+ and K^+ during the gasification of woody and herbaceous biomass. Fig. 3 illustrates the response surfaces of KCl for different levels of independent factors. It indicates that the factor of the equivalence ratio has the major effect on KCl concentration.

The level of KCl dramatically increased by increasing the ER, while it showed a slight decrease by increasing the SB across the whole range of ER. It can be explained by the partial evaporation of solid KCl from the condensed phase at higher temperatures. In addition, according to Norheim et al. [27], this is also caused by the

Table 3
Experimental results and predicted values for the response variables of chlorides distribution.

Run no.	ER	SB	PS (mm)	Exp-HCl (ppmv)	Pre-HCl (ppmv)	Exp-KCl (ppmv)	Pre-KCl (ppmv)	Exp-NaCl (ppmv)	Pre-NaCl (ppmv)	Exp-bottom ash (mg/kg)	Pre-bottom ash (mg/kg)	Exp-fly ash (mg/kg)	Pre-fly ash (mg/kg)
1	0.31	1.4	7.1	2590.7	2684.5	1302.9	1258.7	241.6	250.5	907.3	887.9	2841.5	2771.5
2	0.21	0.9	5.2	1872.4	1804.4	3159.5	3287.6	132.9	126.8	1237.8	1298.3	3287.4	3374.6
3	0.23	1.2	6.5	1512.3	1570.1	2587.6	2497.8	105.8	109.7	1286.2	1239.7	3692.9	3534.2
4	0.36	1.1	8.3	3255.9	3129.8	1187.2	1241.9	369.1	353.1	629.7	654.1	2392.2	2504.9
5	0.27	1.5	7.6	2099.3	2187.9	1841.7	1785.6	182.4	191.3	1072.9	1037.4	3373.5	3236.5

Exp: experimental results; Pre: predicted values.

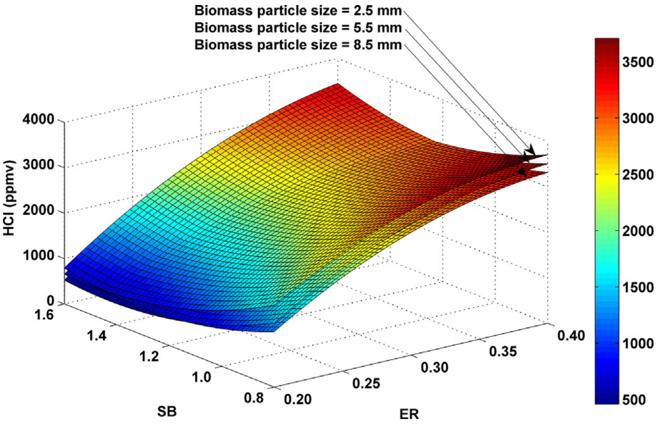

Fig. 2. Response surfaces of HCl for different levels of independent factors.

evaporation of solid and liquid carbonate (K_2CO_3). Besides, the KCl concentration presented a fall after a rise with an increase in biomass particle size at higher air flow rates, which is different from that of HCl.

Compared Fig. 2 with Fig. 3, it was found that the concentration of HCl is always higher than that of KCl in most design spaces, except for the circumstance of lowest level of SB, highest level of ER, and smallest biomass particle size. Norheim et al. [27] investigated the composition of trace compounds from biomass gasification in the solid oxide fuel cell (SOFC) using equilibrium calculations. It was reported that high chlorine content in the fuel favors KCl rather than HCl production. According to Westberg et al. [28], during combustion the biomass with a high moisture content may bring out a high surrounding water-vapor concentration in the gas phase, which may favor the formation of HCl and KOH rather than KCl. It suggests that the feedstock's property is also a key factor determining the release of chlorine in the gasification process. However, as suggested by Kuramochi et al. [29], a linear relationship was not found between the chlorine content of feedstock and HCl concentration. Nevertheless, the relationship could be observed in the relation of sulfur concentration to H_2S during the gasification process. Therefore, it indicates that the distribution of KCl is also concerned with other elements such as heavy metals, alkali and alkaline metals that may retain the chlorine in the condensed phase. The concentration of aluminum and silicon in the feedstock might favor the formation of potassium aluminum silicate compounds instead of KCl. It was reported by Porbatzki et al. [16] that the ratio of (K + Na)/Si and Ca/Si is an important factor that results in the difference in concentrations of HCl and gaseous KCl between the gasification of miscanthus and straw, although the two herbaceous biomass samples have approximately the same amount of chlorine.

3.2.3. Sodium chloride

Fig. 4 shows the response surfaces of NaCl for different levels of independent factors. The factor of ER shows the major influence on the NaCl concentration, whereas SB seems to be relatively less significant for this response variable, compared with variables of HCl and KCl. In terms of the biomass particle size, the content of NaCl slightly increased with an increase in biomass particle size at lower ERs, while the opposite effect can be observed at higher ERs.

As suggested by Norheim et al. [27], the distribution of chlorine between gaseous KCl and NaCl corresponds to the overall ratio of K/Na in the biomass sample. Compared Fig. 3 with Fig. 4, it can be seen that the highest amount of gaseous KCl is approximately ten times higher than that of NaCl, which is nearly consistent with the ratio of K/Na in the fuel. Erbel et al. [30] continuously measured gaseous alkali concentrations in biomass gasification using excimer laser induced fragmentation fluorescence (ELIF). It was observed that the concentration of potassium during gasification of willow is about ten times higher than that of sodium, which is in accordance with the ratio of K/Na of willow. However, he suggested that the dependence of alkali concentration in the feedstock and release content are not proportional for different fuels, even under the same operating conditions. It indicates that the concentration of alkali species is not only concerned with the amount of alkali content.

Overall, it can be seen from Figs. 2–4 that the amount of chlorine released in HCl, gaseous KCl and NaCl increased gradually at higher temperatures brought by higher ERs. In respect to the experimental investigation, Björkman and Strömberg [31] studied the release of chlorine from different biomass fuels (sugarcane trash, switch grass, lucerne and straw) under pyrolysis and gasification conditions. It was found that less than 10% of chlorine had evaporated from the fuel at 200 °C, 20–50% of the total chlorine evaporated at 400 °C, while 30–60% of the chlorine was still left in the char at 900 °C. In terms of theoretical research, Turn [21] used chemical equilibrium calculations to predict the trace species K, Na and Cl in the product gas from gasification of banagrass. It was reported that the Cl was found to increase dramatically from 700 ppmw to around 2400 ppmw at lower temperatures, and then increased gradually at higher temperatures. In terms of K, it was found to increase dramatically from 200 ppmw to approximately 1100 ppmw at lower temperatures and then increased gradually at higher temperatures. As for the concentration of Na, it was observed to increase from 0 ppmw to about 200 ppmw. Konttinen

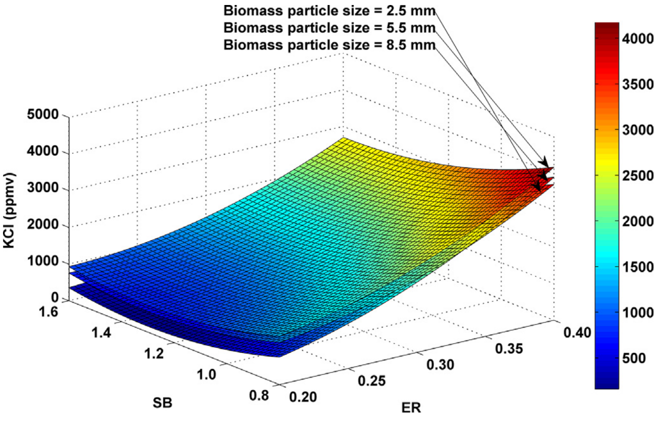

Fig. 3. Response surfaces of KCl for different levels of independent factors.

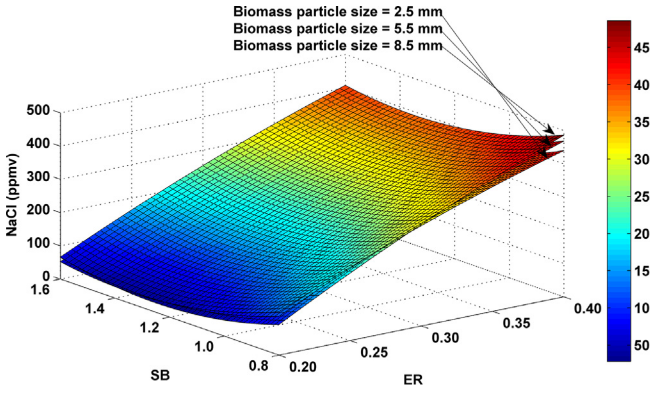

Fig. 4. Response surfaces of NaCl for different levels of independent factors.

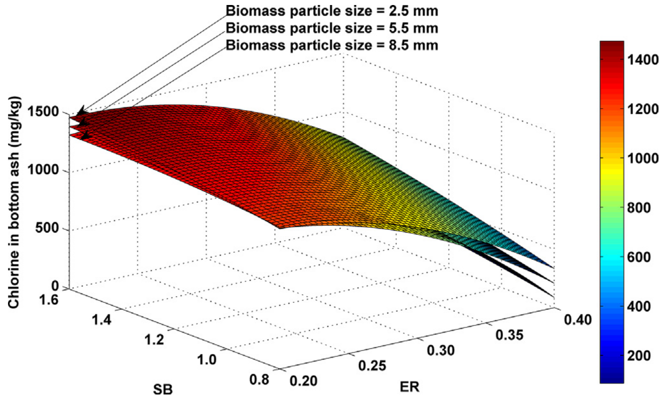

Fig. 5. Response surfaces of chlorine retained in the bottom ash for different levels of independent factors.

et al. [32] identified the behavior of gaseous chlorine and alkali metals during biomass gasification by the method of thermodynamic equilibrium calculations. It was observed the same behavior of K, Cl and Na released in gas phase as a function of gasification temperature increasing from 600 to 1000 °C. Therefore, taking into account the differences in the experimental systems and the feedstock properties, the result in this study showed similar trends to those obtained in the literature. In addition, it can be observed from Figs. 2–4 that equivalence ratio is the most influential factor affecting the chlorine retained in the gaseous phase. Besides, the effect of steam to biomass mass ratio on chlorine bounded in the condensed phase is greater than that of biomass particle size.

3.3. Chlorides bounded in the condensed phase

3.3.1. Chlorine bounded in the bottom ash

Fig. 5 shows the response surfaces of chlorine bounded in the bottom ash for different levels of independent factors. This figure and Table 2 indicate that the amount of chlorine bounded in the bottom ash is comparatively more dependent on the factor of ER, instead of SB and biomass particle size.

Increasing the ER could dramatically decrease the chlorine concentration in the bottom ash. For lower ERs, this response variable showed a slight increase with increasing the SB, while this positive effect is pronounced at higher ERs. It can be explained by the fact that the reactor temperature increases with increasing the ER and decreasing the SB. Then some inorganic chlorides such as KCl and NaCl retained in the solid ash are more released as gaseous chlorine species. Besides, it can also be observed that the negative effect of biomass particle size can be negligible at lower ERs and lower levels of SB, whereas this effect is obvious at any other operating conditions and pronounced at higher ERs and higher levels of SB.

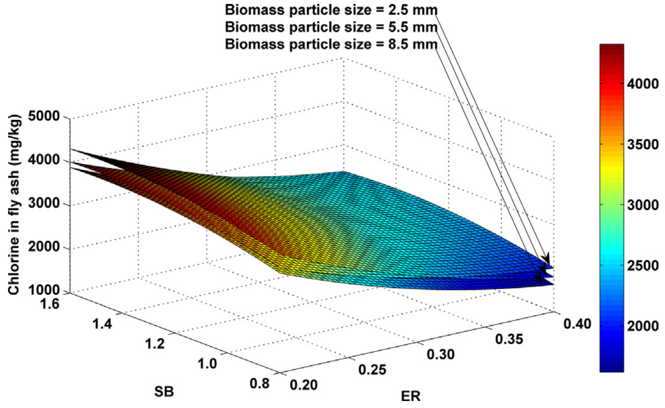

Fig. 6. Response surfaces of chlorine retained in the fly ash for different levels of independent factors.

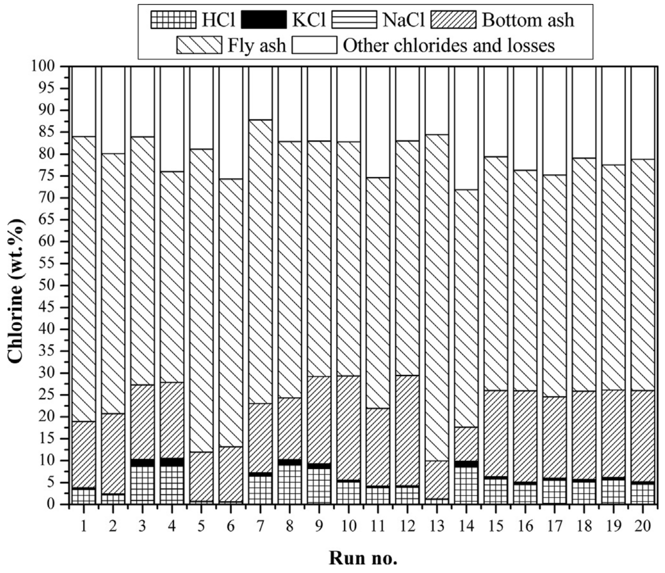

Fig. 7. Distribution of chlorine in the product streams during the gasification process.

3.3.2. Chlorine bounded in the fly ash

Fig. 6 demonstrates the response surfaces of chlorine bounded in the fly ash for different levels of independent factors. It shows that this response variable depends significantly on the three factors and their interactions. The content of chlorine in the fly ash continuously decreased with an increase in the ER, and this negative effect is more pronounced at a lower level of SB. For lower ERs, this response variable increased gradually with increasing the SB, and this negative effect can be negligible at higher ERs. The unparallel surfaces generated indicate that the effect of biomass particle size is different within the design space. At lower ERs, the chlorine concentration in the fly ash increased first and then decreased with increasing the biomass particle size, while at higher ERs the chlorine concentration in the fly ash decreased gradually with the increment of biomass particle size.

Overall, it can be seen from Figs. 5 and 6 that equivalence ratio still plays a leading role in affecting the chlorine retained in the condensed phase. Besides, the effect of biomass particle size on chlorine bounded in the condensed phase is greater than that of steam to biomass mass ratio. It can also be observed that the concentration of chlorine in the fly ash is about two times higher than that of bottom ash within the design space. Since the temperature of fly ash collected in the ash hopper 2 at the bottom of the cyclone is lower than the temperature of bottom ash collected in the ash hopper 1 at the bottom of the reactor. Therefore, the gaseous inorganic chlorides (KCl and NaCl) in the product gas condense on the solid ash particles at the bottom of the cyclone, resulting in a relatively higher amount of chlorine in the fly ash.

3.4. Chlorine mass balance

Fig. 7 shows the distribution of chlorine in gaseous products and retained in solid ashes. Throughout all the tests, it can be clearly seen that depending on the operation conditions during the gasification process, a substantial fraction, up to 60–80 wt%, of the chlorine in the feedstock were retained in the ashes, especially in fly ashes. A small amount of chlorine was transformed into gaseous chlorides, which didn't exceed 10 wt% of the total chlorine. And the gaseous chlorides were mainly released as HCl. A tiny amount of chlorine could be observed in alkali salts such as KCl and NaCl. According to the mass balance of sulfur investigated in the previous study [33], it was observed that 25–35 wt% of the sulfur were retained in the ashes, while a substantial fraction, 30–60 wt%, of the sulfur in the feedstock were released into gaseous sulfides, depending on the operation conditions. Therefore, it can be seen that chlorine species have different distribution during the gasification of non-woody biomass compared with that of sulfur, which may be affected by different chemistry of the two elements.

The mass balance of chlorine was not closed. Fig. 4 shows around 10–30 wt% of the total chlorine could not be specifically determined in this study. The main reason for the incomplete chlorine balance is that a considerably amount of chlorine could not be measured due to the accumulation of ash in the installations, including the reactor and cyclone. Besides, the lost mass of chlorine in the feedstock probably went to other chemical compounds such as gaseous dioxins and chlorides in aerosol particles, which may result in a certain amount of mass loss of chlorine.

4. Conclusions

Non-woody biomass gasification experiments based on response surface methodology shows that the three operating parameters (equivalence ratio, steam to biomass mass ratio and biomass particle size) significantly affected the distribution of chlorine species in the gaseous phase and the condensed phase. It was found that the three operating parameters have different influence on the five response variables. In terms of the effect of the equivalence ratio, a corresponding increase gave rise to the increase of gaseous chlorine (i.e. HCl, KCl and NaCl) and the decrease of chlorine in the ashes (i.e. bottom ash and fly ash). As for the effect of steam to biomass mass ratio, a corresponding increase resulted in the decrease of KCl and NaCl as well as the increase of chlorine in bottom and fly ash. In addition, the concentration of HCl rose again after a fall. In respect to the effect of biomass particle size, a corresponding increase resulted in the decrease of HCl and chlorine in the bottom ash, while the concentration of KCl underwent the process of a fall after a rise. Besides, with increased biomass particle size, the concentration of NaCl increased and the chlorine in fly ash decreased at higher ERs. At lower ERs, the concentration of NaCl decreased while the chlorine in fly ash presented a decrement after an increment. The relation of K/Na in the fuel is relevant for the relation of gaseous KCl/NaCl produced during the gasification process.

Acknowledgments

Financial support for this study that has been provided by Shandong Provincial Natural Science Foundation of China (no. 2009ZRA01100 and ZR2009EZ001) and National Science and Technology support program (2010BAC66B02, 2011BAD15B05-05 and 2011YQ120039) is gratefully acknowledged.

References

[1] Erlach B, Harder B, Tsatsaronis G. Combined hydrothermal carbonization and gasification of biomass with carbon capture. Energy 2012;45:329–38.

[2] Johansson MT. Bio-synthetic natural gas as fuel in steel industry reheating furnaces – a case study of economic performance and effects on global CO_2 emissions. Energy 2013;57:699–708.

[3] Kim BH, Lee S, Maken S, Song HJ, Park JW, Min B. Removal characteristics of PCDDs/Fs from municipal solid waste incinerator by dual bag filter (DBF) system. Fuel 2007;86:813–9.

[4] Park K, Hyun H, Maken S, Jang S, Park JW. Vitrification of municipal solid waste incinerator fly ash using brown's gas. Energy Fuels 2005;19:258–62.

[5] Biomass program multi-year program plan. URL: http://www1.eere.energy.gov/biomass/pdfs/mypp_april_2012.pdf; April 2012.

[6] Li XT, Grace JR, Lim CJ, Watkinson AP, Chen HP, Kim JR. Biomass gasification in a circulating fluidized bed. Biomass Bioenergy 2004;26:171–93.

[7] Kotowicz J, Sobolewski A, Iluk T. Energetic analysis of a system integrated with biomass gasification. Energy 2013;52:265–78.

[8] Hathaway BJ, Honda M, Kittelson DB, Davidson JH. Steam gasification of plant biomass using molten carbonate salts. Energy 2013;49:211–7.

[9] Kwak TH, Lee S, Maken S, Shin HC. A study of gasification of municipal solid waste using a double inverse diffusion flame burner. Energy Fuels 2005;19:2268–72.

[10] Hernández JJ, Ballesteros R, Aranda G. Characterisation of tars from biomass gasification: effect of the operating conditions. Energy 2013;50:333–42.

[11] Kwak TH, Maken S, Lee S, Park JW, Min BR, Yoo YD. Environmental aspects of gasification of Korean municipal solid waste in a pilot plant. Fuel 2006;85:2012–7.

[12] Kwak TH, Lee S, Park JW, Maken S, Yoo YD, Lee SH. Gasification of municipal solid waste in a pilot plant and its impact on environment. Korean J Chem Eng 2006;23:954–60.

[13] Batidzirai B, Mignot APR, Schakel WB, Junginger HM, Faaij APC. Biomass torrefaction technology: techno-economic status and future prospects. Energy 2013;62:196–214.

[14] Nzihou A, Flamant G, Stanmore B. Synthetic fuels from biomass using concentrated solar energy – a review. Energy 2012;42:121–31.

[15] Gai C, Dong YP. Experimental study on non-woody biomass gasification in a downdraft gasifier. Int J Hydrogen Energy 2012;37:4935–44.

[16] Porbatzki D, Stemmeler M, Müller M. Release of inorganic trace elements during gasification of wood, straw, and miscanthus. Biomass Bioenergy 2011;5:S79–86.

[17] DeMartini AAN, Pranovich A, Krogell J, Kumar N, Eränen K, Holmbom B, et al. Pyrolysis of pine and gasification of pine chars – influence of organically bound metals. Bioresour Technol 2013;128:22–9.

[18] Yang Y, Jin S, Lin Y, Huang S, Yang H. Catalytic gasification of tobacco rob in steam–nitrogen mixture: kinetic study and the fuel gas analysis. Energy 2012;44:509–14.

[19] Valero A, Usón S. Oxy-co-gasification of coal and biomass in an integrated gasification combined cycle (IGCC) power plant. Energy 2006;31:1643–55.

[20] Fermoso J, Gil MV, Arias B, Plaza MG, Pevida C, Pis JJ, et al. Application of response surface methodology to assess the combined effect of operating variables on high-pressure coal gasification for H_2-rich gas production. Energy 2010;35:1191–204.

[21] Turn SQ. Chemical equilibrium prediction of potassium, sodium, and chlorine concentrations in the product gas from biomass gasification. Ind Eng Chem Res 2007;46:8928–37.

[22] Ellwood MJ, Hunter KA, Cunninghame RG. Elimination of equivalence point errors in the potentiometric titration of chloride, bromide and iodide mixtures with silver nitrate. Microchem J 2003;74:187–92.

[23] Raghunathan K, Gullett BK. Role of sulfur in reducing PCDD and PCDF formation. Environ Sci Technol 1996;30:1827–34.

[24] Pinto F, André RN, Lopes H, Dias M, Gulyurtlu I, Cabrita I. Effect of experimental conditions on gas quality and solids produced by sewage sludge cogasification. 2. Sewage sludge mixed with biomass. Energy Fuels 2008;22:2314–25.

[25] Wei X, Schnell U, Hein KRG. Behaviour of gaseous chlorine and alkali metals during biomass thermal utilization. Fuel 2005;84:841–8.

[26] Aljbour SH, Kawamoto K. Bench-scale gasification of cedar woody – part II: effect of operational conditions on contaminant release. Chemosphere 2013;90:1501–7.

[27] Norheim A, Lindberg D, Hustad JE, Backman R. Equilibrium calculations of the composition of trace compounds from biomass gasification in the solid oxide fuel cell operating temperature interval. Energy Fuels 2009;23:920–5.

[28] Westberg HM, Byström M, Leckner B. Distribution of potassium, chlorine, and sulfur between solid and vapor phases during combustion of wood chips and coal. Energy Fuels 2003;17:18–28.

[29] Kuramochi H, Wu W, Kawamoto K. Prediction of the behaviors of H_2S and HCl during gasification of selected residual biomass fuels by equilibrium calculation. Fuel 2005;84:377–87.

[30] Erbel C, Mayerhofer M, Monkhouse P, Gaderer M, Spliethoff H. Continuous in situ measurements of alkali species in the gasification of biomass. Proc Combust Inst 2013;34:2331–8.

[31] Björkman E, Strömberg B. Release of chlorine from biomass at pyrolysis and gasification conditions. Energy Fuels 1997;11:1026–32.

[32] Konttinen J, Backman R, Hupa M, Moilanen A, Kurkela E. Trace element behavior in the fluidized bed gasification of solid recovered fuels – a thermodynamic study. Fuel 2013;106:621–31.

[33] Gai C, Dong YP, Zhang T. Distribution of sulfur species in gaseous and condensed phase during downdraft gasification of corn straw. Energy 2014;64:248–58.